Proceedings of ICRC 2001: 649 © Copernicus Gesellschaft 2001

ICRC 2001

Cloud detection at the High Resolution Fly's Eye

R. W. Clay, B. R. Dawson, R. T. Pace, D. S. Riordan, A. G.K. Smith, N. R. Wild, and the HiRes Collaboration

Physics Department, University of Adelaide, Adelaide SA 5005, Australia

Abstract. The presence of cloud can adversely affect many ground-based astrophysics observations. In the HiRes experiment, where fluorescence light is detected from distant air showers, cloud must be monitored over a large part of the night sky. Solid layers of cloud reduce the fiducial volume available to the detector, while broken cloud can block light from part of a shower track, giving structure to the light signal that may be misinterpreted. To tackle these problems we have developed two versions of infra-red cloud detectors, both based on an inexpensive commercial sensor. First, we employ a number of fixed devices that each monitor a rather large field of view (30° diameter) around the horizon, searching for cloud in the directions viewed by our fluorescence mirrors. The other type is a small field of view (3°) detector mounted on a pan-and-tilt platform that continously scans the entire night sky.

1 Introduction

Night-time cloud is detectable via the blackbody radiation that it emits. The cloud, in thermal equilibrium with the air at a particular height, appears warm against the background clear sky. The amount of contrast between clear and cloudy sky depends on the wavelength band selected, the optical depth (or emissivity) of the cloud and the intensity of emission from clear sky. The latter typically depends on the amount of water vapour in the atmosphere since water radiates in the far-IR where cloud is typically brightest. Contrast between clear sky and cloud is less at large zenith angles where the integrated water vapour signal is largest.

The operation of infra-red cloud detectors in high energy astrophysics has been described by Clay et al. (1998) and Buckley et al. (1999).

We have installed two types of cloud detector at the HiRes-1 site in the western desert of Utah (HiRes Collaboration, 2001). Both are based on the same commercial IR sensor (EG&G Heimann TPS 534), a thermopile sensitive in the $5.5-20\mu$m band. This passband is reduced to approximately $7-13\mu$m by the plastic covers and lenses used in our devices. The electronic circuitry in both detectors is very similar and is described in Clay et al. (1998). The sensor responds to the temperature difference between the sensitive thermopile element, which is in thermal equilibrium with a pre-determined field of view, and the detector canister whose temperature is measured with an internal thermistor.

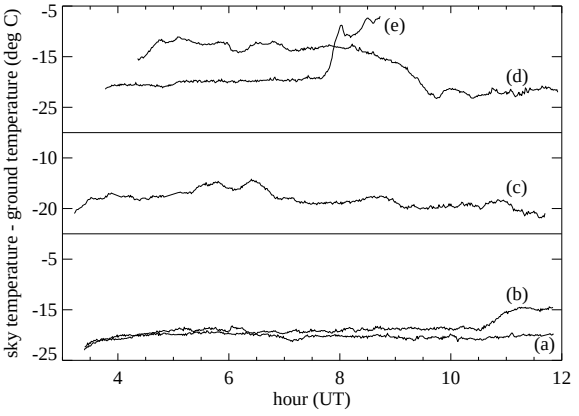

Fig. 1. Examples of horizon cloud monitor signals from Dugway in March/April 1999 (Clay et al., 1999). Each line represents the difference between the measured sky temperature and that of the detector canister, the latter being close to the ground temperature. Large negative values represent clear skies.

Our "horizon monitors" are mechanically collimated by an aluminium tube to limit the diameter of their fields of view (FOV) to approximately 30°. The end of each tube is covered with IR-transmitting polyethylene (manufactured by COIL). We have installed 11 such devices at the HiRes-1 site to view 330° of horizon up to 30° elevation. The devices are mounted in mirror buildings and we use the HiRes data

Correspondence to: B. Dawson
(bdawson@physics.adelaide.edu.au)

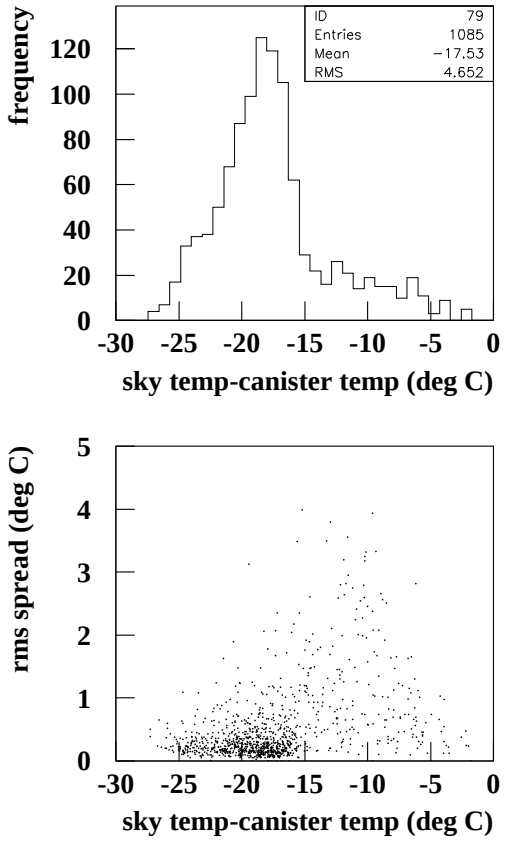

Fig. 2. Data from more than 1000 hours of operation of a single horizon cloud monitor. The top plot shows the temperture averaged over one hour periods, and the bottom plot shows how this mean is correlated with the rms variation within each hour.

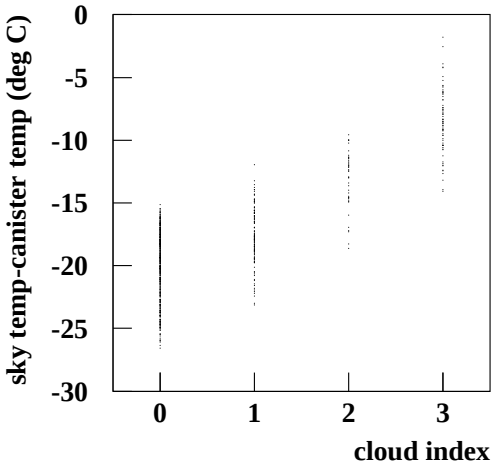

Fig. 3. The cloud index for our horizon monitors takes into account the measured sky temperature (w.r.t. the ground temperature) and the dew point. A zero indicates no cloud in the FOV (63% of data); 1 means a little low cloud or a larger area of very high cloud in the FOV (20% of data); 2 means moderate amount of low cloud in the FOV (6% of data); and 3 means overcast low cloud in the FOV (11% of data).

acquisition electronics to read the IR sensor voltages every minute during HiRes operation. The full complement of detectors has been in place since August 1999.

We have also constructed a "scanning" cloud monitor. Here we have used a plastic fresnel lens (Kube model 1010) to limit the sensor FOV to approximately 3° diameter. The detector has been mounted on a pan-and-tilt platform (ULTRAK PT-325) that allows us to scan the entire sky every 12 minutes. The scan time is determined primarily by the effective integration time of the IR sensor (approximately $0.2\,\mathrm{s}$) and the number of independent 3° diameter areas on the sky (approximately 3000). We have developed software to drive the pan-and-tilt platform and display the IR image of the sky. The scanner, mounted at HiRes-1, has been monitoring the sky during HiRes operation since March 2001.

2 Measurements from the Horizon Cloud Monitors

Figure 1 shows some horizon cloud monitor data from Clay et al. (1999). The temperature displayed is the effective sky temperature minus the detector canister temperature, the latter being close to ground temperature. This definition attempts to remove the effect of a changing atmospheric temperature, the assumption being that the ground temperature sets the reference point for the atmospheric temperature profile. This renormalized sky temperature should then be, to first order, dependent on the cloud height, the cloud emissivity and the fraction of FOV covered by cloud. Cold temperatures represent clear sky, and warm temperatures (near 0°C) indicate low, thick cloud. In Figure 1, traces (a) and (b) represent clear nights (with some haze towards the end of (b)), trace (c) represents a night with variable cloud, trace (d) is a cloudy night with improvement later in the night, and trace (e) is a mostly clear night where cloud rolled in during the final hour. We have confirmed that the cloud monitors are superior to the infrequent observations by the HiRes operator (Clay et al., 1999).

In Figure 2 we show summary data from one of the horizon monitors for over 1000 hours of night-time operation. The first histogram shows the hourly-averaged sky temperature, measured with respect to the detector canister temperature (as before). The plot indicates a range of temperatures from less than -20°C (clear sky) to near 0°C (low thick cloud). Note that this is a biased sample of conditions since the cloud

Fig. 4. The scanning cloud monitor in Salt Lake City during testing. Our IR detector views the sky through a fresnel lens limiting its FOV to a diameter of 3°. The pan-and-tilt platform is computer controlled and we image the full sky every 12 minutes.

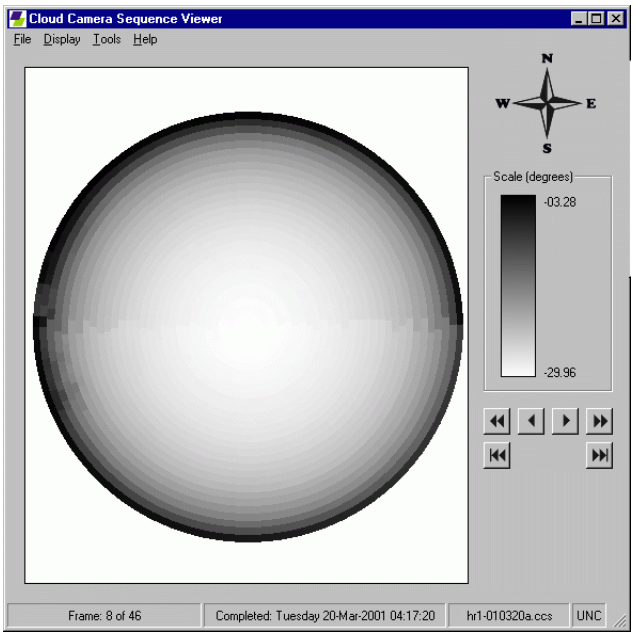

Fig. 5. Full-sky image from the scanning cloud monitor at HiRes in March 2001. This image shows a sky free of cloud. The variation in temperature (here defined as sky temperature minus ground temperature) from the zenith to the horizon is obvious. The grey scale ranges from a temperature of approx -30°C (white) to -3°C (black).

monitors only operate when the HiRes detector is collecting data. Figure 2(b) shows a correlation between the mean sky temperature and its rms value, calculated hourly. This illustrates that when cloud exists, it often shows variability over a period of an hour.

As mentioned earlier, the clear sky temperature has some dependence on the atmosphere's water content. On humid nights the clear sky temperature is raised by up to 8°C in the low elevation ($< 30^\circ$) area of sky viewed by the monitors. We have developed a procedure to make a correction to the cloud monitor reading based on the air temperature and dew point. A 4-value "cloud index" is then calculated which indicates the likelihood of cloud within each detector's FOV. This index is plotted in Figure 3 against the sky temperature. The index is used to make data quality cuts for analysis. In addition, full records of cloud monitor readings are maintained for use in the analysis of significant air shower events.

3 Measurements from the Scanning Cloud Monitor

The scanning cloud monitor is shown in Figure 4. The detector is the same used in the horizon monitors, but is housed behind a plastic fresnel lens which defines a 3° diameter FOV.

Figure 5 shows an image of the full sky on a night with no cloud. Again, the temperature plotted is the sky temperature minus the detector canister temperature, and it ranges from -30°C at the zenith to -3°C near the horizon, a consequence of an increasing optical depth of radiating molecules (particularly water) within the bandpass of the detector.

Figure 6 shows an image from later the same night when some cloud has appeared. While cloud is obvious in this picture, it is more obvious when the temperature of the clear sky (including its zenith angle dependence) is subtracted. This is shown in Figure 7, which displays the difference between temperatures in Figure 5 and Figure 6.

Twelve minutes later the cloud has increased further. This is shown in Figures 8 and 9.

Data from this monitor will be used to more accurately detemine the direction of small clouds within the HiRes detection volume. Another identical detector is planned for the second HiRes site 13 km away.

4 Conclusion

We have developed a complete system for monitoring cloud at the High Resolution Fly's Eye site in Utah. A combination of wide FOV horizon monitors with a narrow FOV scanner provides immediate feedback to the detector operators on the state and progression of cloud cover, as well as providing a record of cloud conditions to be used in event analysis.

Acknowledgements. The cooperation of Colonel Fisher and staff of the US Army Dugway Proving Grounds is gratefully acknowledged. This work is supported by the US National Science Foundation, the US Department of Energy, and the Australian Research Council.

References

Buckley, D.J. et al., Experimental Astronomy, 9, 237–249, 1999.
Clay, R.W. et al., Publ. Ast. Soc. Aust., 15, 332–335 1998.
Clay, R.W. et al, Proc. 26th ICRC, Salt Lake City, 5, 421–424, 1999.
HiRes Collaboration, "Description of the High Resolution Fly's Eye Detector, HE1.4.1 these proceedings, 2001.

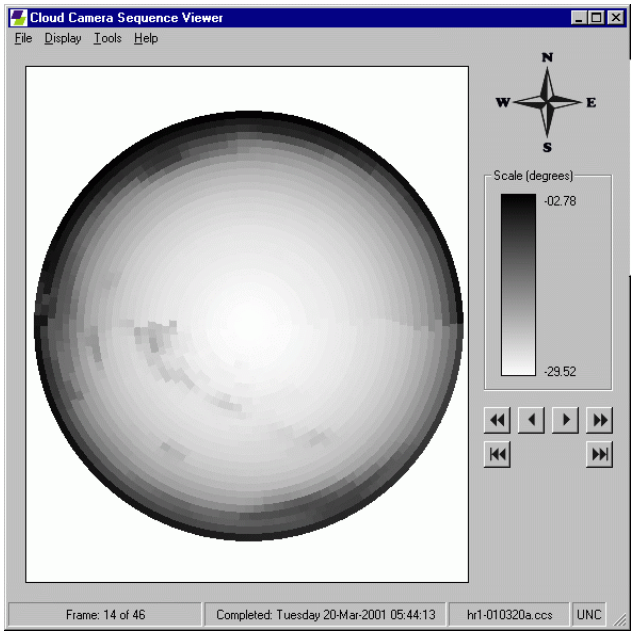

Fig. 6. Full-sky image from the cloud monitor showing cloud.

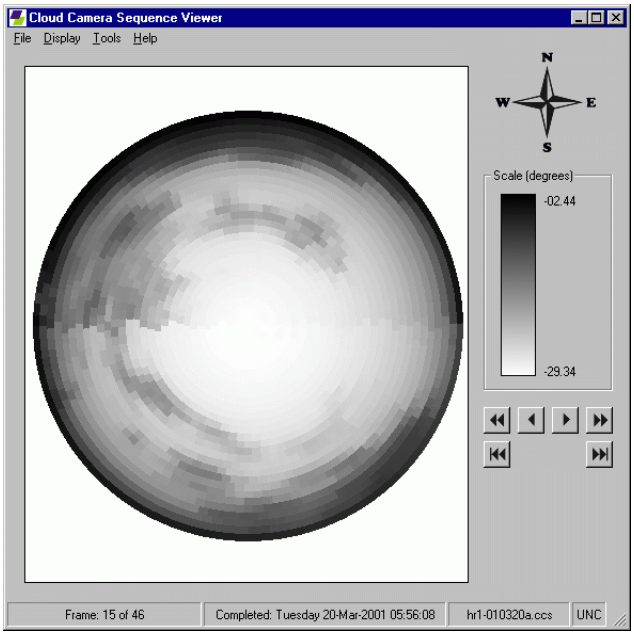

Fig. 8. Twelve minutes later the cloud has increased further.

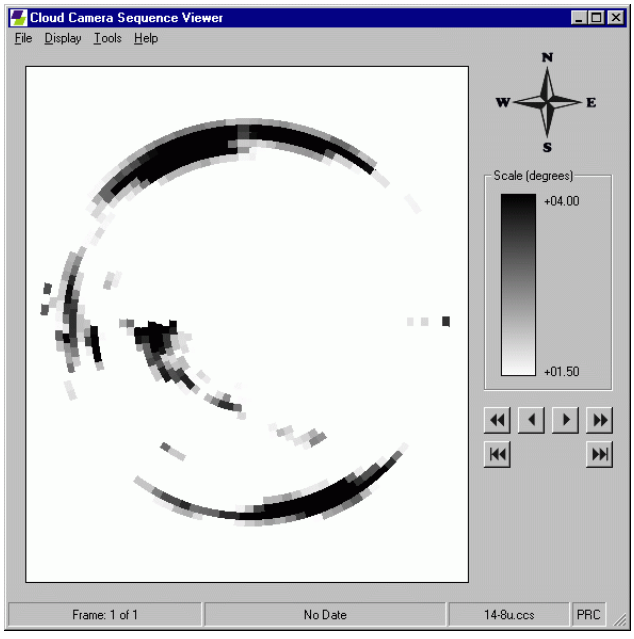

Fig. 7. The same image as above, but with the temperature of the clear sky subtracted, including its zenith dependence. The scale (1.5° to 4°C) shows the temperature of the cloud with respect to the clear sky.

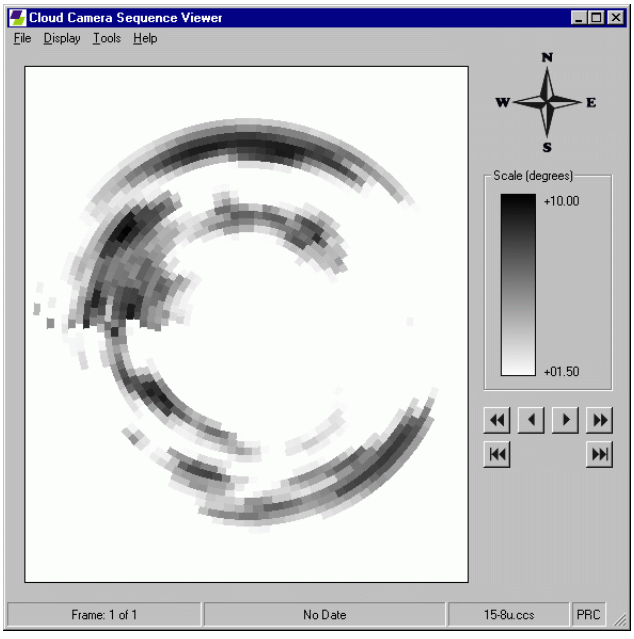

Fig. 9. Full-sky image from the figure above with the clear sky temperature subtracted. Here we have expanded to temperature scale to 1.5° to 10°C to show more clearly some variations in cloud temperature.